New Monte Carlo method to compute the free energy of arbitrary solids. Application to the fcc and hcp phases of hard spheres

Daan Frenkel
Fysisch Laboratorium, Rijksuniversiteit Utrecht, P.O. Box 80000, 3508 TA Utrecht, The Netherlands
Anthony J. C. Ladd[a)]
Department of Applied Science, University of California at Davis, Davis, California 95616

(Received 14 March 1984; accepted 18 April 1984)

We present a new method to compute the absolute free energy of arbitrary solid phases by Monte Carlo simulation. The method is based on the construction of a reversible path from the solid phase under consideration to an Einstein crystal with the same crystallographic structure. As an application of the method we have recomputed the free energy of the fcc hard-sphere solid at melting. Our results agree well with the single occupancy cell results of Hoover and Ree. The major source of error is the nature of the extrapolation procedure to the thermodynamic limit. We have also computed the free energy difference between hcp and fcc hard-sphere solids at densities close to melting. We find that this free energy difference is not significantly different from zero: $-0.001 < \Delta F < 0.002$.

INTRODUCTION

In this paper we present a computer simulation method to determine the domain of thermodynamic stability of solid phases. The recent development by Parinello and Rahman[1] of a new molecular dynamics simulation technique have stimulated the use of computer simulations in investigating solid–solid phase transitions in model systems. The idea upon which the Parinello–Rahman method is based is that the fixed periodic boundary conditions employed in conventional MD simulations exclude the direct observation of solid–solid phase transitions, as the boundary conditions chosen to be compatible with one solid phase are, in general, incompatible with the other. Hence, fixed periodic boundary conditions tend to stabilize one solid phase well beyond its range of thermodynamic stability, and may easily overlook the existence of other more stable phases altogether. In the Parinello–Rahman method the shape of the periodic box is no longer fixed; shape and size of the periodic box are expressed in terms of variables which play the role of generalized coordinates in an extended Hamiltonian. The resulting equations of motion describe the "natural" time evolution of the shape and size of the periodic box under constant applied external pressure and zero applied stress. The Parinello–Rahman method provides a "reaction path" from one solid phase to the other as the boundary conditions adjust themselves to the favored solid structure. For this reason this method is now being used to map phase diagrams involving several solid phases (see e.g., Refs. 2 and 3). It should be noted however that the method does not provide a *reversible* route from one solid phase to the other; the solid–solid phase transformation takes place when the initial solid phase becomes mechanically unstable. The actual thermodynamic phase transition is bracketed by the width of the hysteresis region. In order to locate the thermodynamic phase transition precisely one needs information on the free energy of both solid phases.

Two methods have traditionally been used to obtain such information. Both methods rely on the construction of a reversible path from a state of known free energy to the solid phase under consideration. The first method is the single occupancy cell (SOC) method introduced by Hoover and Ree.[4] This method starts with a lattice gas with one particle per lattice cell. At high densities the centers of the lattice cells coincide with the average atomic positions in the unconstrained solid. Expanding this lattice uniformly leads to a dilute gas which has the same pressure as an ideal gas at the same density, and a free energy that can be evaluated exactly. The free energy of the lattice gas at high densities coincides with the free energy of the corresponding unconstrained solid, provided that the density is sufficiently high to ensure that the artificial cell walls have negligible effect on the particle displacements. The free energy of the solid is then obtained by computing

$$F_{\text{solid}}(V_2) - F_{\text{lattice gas}}(V_1) = -\int_{V_1}^{V_2} P(V)dV \qquad (1)$$

at constant temperature. This method was used by Hoover and Ree to obtain the absolute free energy of the hard-sphere and hard-disk solids.[4,5] The actual numerical integration of Eq. (1) may require evaluating the pressure at many state points because lattice-gas isotherms exhibit a cusp at the point where the nearest-neighbor interactions take over from the cell walls in constraining the particles. There is even some evidence that a weak first-order transition takes place at this point,[6] in which case, the supposedly reversible path linking the solid to the dilute lattice gas may not be quite reversible, after all.

A second method of computing the free energy of a solid phase is to start from the low-temperature harmonic solid, the free energy of which can be computed exactly. This method was first used by Hoover, Gray, and Johnson.[7] There are two factors limiting the applicability of the latter method. The first is that it only works for solids which are harmonic at low temperatures (and/or high densities). This excludes all systems with discontinuous intermolecular

a) Present address: Lawrence Livermore National Laboratory L-454, Livermore, California 94550.

 0021-9606/84/193188-06$02.10

forces, e.g., the hard-sphere solid. Moreover, solid phases that are mechanically unstable at low temperatures cannot be investigated by this method. A practical problem with the harmonic-lattice method is that for all but the simplest solids, and in particular for molecular solids, evaluating the harmonic lattice free energy involves lengthy computation.

METHOD

In this section we introduce a new method to compute the absolute free energy of a solid phase. Our approach is once again based on the construction of a reversible path to a state of known free energy. In this case the reference state is an Einstein crystal with the same structure as the solid under consideration. This reference state can be reached from the real solid by slowly switching on harmonic springs which bind the atoms to their lattice sites. As the Einstein solid is structurally identical to the initial solid, it is very likely that such a path will be free of phase transitions and hence reversible. The simplest way to transform a solid to an Einstein crystal is to add a term λV to the unperturbed Hamiltonian H_0, such that

$$H(\lambda) = H_0 + \lambda V = H_0 + \lambda \sum_{i=1}^{N} (\mathbf{r}_i - \mathbf{r}_i^0)^2, \tag{2}$$

where $\mathbf{r}_i^0$ is the lattice position of particle i. The derivative of the free energy of this system with respect to the coupling constant λ is given by

$$\frac{\partial F}{\partial \lambda} = -kT \frac{\partial}{\partial \lambda} \left\{ \ln \int \cdots \int \exp[-\beta(H_0 + \lambda V)] d\mathbf{q}^N \right\} = \langle V \rangle_\lambda, \tag{3}$$

from which it follows that the free energy of the real crystal is related to the free energy of a crystal with spring constant λ by

$$F(\lambda = 0) = F(\lambda) - \int_0^\lambda \langle V \rangle_{\lambda'} d\lambda'. \tag{4}$$

At sufficiently high λ the free energy of the system reduces to that of an Einstein crystal

$$F(\lambda) = \Phi_0 - kT \ln(\pi kT/\lambda)^{3N/2} + C(T) + O(1/\lambda), \tag{5}$$

where Φ_0 is the potential energy of the corresponding static lattice. $C(T)$ is the kinetic contribution to the free energy which depends only on the temperature T. Of course, a rather high value of λ may be required before terms of order $O(1/\lambda)$ in Eq. 5 become negligible. In practice there is no need to go to very high values of λ as it is rather simple to evaluate the leading corrections to the free energy at finite λ. In some cases these corrections can be evaluated analytically, as in the case of hard spheres to be discussed below, but in the most general case the free energy difference between the ideal Einstein crystal and the Einstein crystal with intermolecular interactions (henceforth referred to as the interacting Einstein crystal) can be found numerically by performing a Monte Carlo simulation on the ideal Einstein crystal, and deriving the free energy of the interacting Einstein crystal by umbrella sampling.[8] Depending on the nature of the system studied it may be useful to parametrize the Hamiltonian in a different way. For instance, for systems with continuous intermolecular interactions one may switch on the spring constants while switching off the intermolecular interactions. In general, the Hamiltonian may depend on λ in a nonlinear fashion. Equation (4) then becomes

$$F(\lambda = 0) = F(\lambda) - \int_0^\lambda \left\langle \frac{\partial H(\lambda')}{\partial \lambda'} \right\rangle d\lambda'. \tag{4a}$$

By a suitable choice of the parametrization of $H(\lambda)$ one may achieve a situation where $|\langle \partial H/\partial \lambda' \rangle|$ is quite small for $0 \leqslant \lambda' \leqslant \lambda$. Such a parametrization corresponds to a situation where the free energy of the Einstein crystal is quite close to the free energy of the initial crystal. It is likely that such a parametrization will result in an improved accuracy of the free energy computation. This method is also applicable to solids containing defects, particularly grain boundaries. The reference lattice in this case is the fully relaxed lattice containing the defect.

APPLICATION TO THE HARD-SPHERE SOLID

In order to test the usefulness of the method described above we used it to compute the free energy of the fcc and hcp phases of the hard-sphere solid at two densities close to the solid–fluid coexistence point. We chose this particular system for two reasons: First, of all reliable numerical results on the free energy of the fcc phase of the hard sphere solid are available,[5] yet the calculations on which these results are based are by no means trivial; they involve the computation of a complete isotherm of the single-occupancy cell system. Secondly, the old question of the relative stability of the hcp and fcc phases of the hard-sphere solid at melting is, thus far, unresolved. There is some evidence that as the solid density approaches ρ_0, the density of closest packing, the fcc phase is the more stable,[9–11] but as the pressure of the dense hcp phase is slightly higher than the pressure of the fcc phase,[10] it is not obvious which phase is the more stable at the melting point. In the present study we have computed the free energy of both fcc and hcp solids at a reduced density $\rho/\rho_0 = 0.7360$ (i.e., the density of the solid at the solid–fluid coexistence point, according to Ref. 5) and at a slightly higher density $\rho/\rho_0 = 0.7778$. Each simulation consisted of ten runs, for different values of the spring constant λ. Every run consisted of at least 10^4 sweeps (i.e., 10^4 attempted moves per particle) excluding equilibration; many runs were appreciably longer. The values of λ at which the different runs were carried out were chosen as follows. For $\lambda > \lambda_{max}$ ($\lambda_{max} \simeq 632$ for $\rho/\rho_0 = 0.7360$, and $\lambda_{max} \simeq 1775$ for $\rho/\rho_0 = 0.7778$) the free energy of the interacting Einstein crystal could be accurately approximated by an analytical expression based on a "virial-like" cluster expansion, described in the Appendix. Hence, the numerical simulations were limited to the interval $0 < \lambda < \lambda_{max}$. The mean-square particle displacement $\langle r^2 \rangle$, which is the integrand in Eq. (4), depends strongly on λ. At high values of λ, $\langle r^2 \rangle \sim 1/\lambda$ whereas as $\lambda \to 0$, $\langle r^2 \rangle \to \langle r^2 \rangle_0$, the mean-square displacement of an atom around its lattice site in the normal hard-sphere solid. Clearly, the function $(\lambda + c)\langle r^2 \rangle$ varies much less over the interval $0 < \lambda < \lambda_{max}$, if we choose $c \simeq kT\sigma^2/\langle r^2 \rangle_0$. We make use of this fact to transform the integral in Eq. (4) in such a way that the integrand becomes a slowly varying function of the integration vari-

able. To this end we write the integral in Eq. (4), i.e., the free energy difference between the interacting Einstein crystal and the hard-sphere solid as

$$\Delta F = -\int_0^{\lambda_{\max}} \langle r^2\rangle_\lambda (\lambda + c)\frac{d\lambda}{(\lambda + c)}$$
$$= -\int_{\ln(c)}^{\ln(\lambda_{\max}+c)} \{\langle r^2\rangle_\lambda (\lambda + c)\} d\ln(\lambda + c). \quad (6)$$

Here the integrand is a very smooth function of $\ln(\lambda + c)$ [we chose $c = \exp(3.5)$], and the integral could be evaluated using a 10-point Gauss–Legendre quadrature.[12] Later tests indicated that no significant loss of accuracy resulted if a five-point quadrature was used. A typical simulation consisting of ten runs of 10^4 sweeps for a 108 particle system took about 20 min on an IBM 192 computer.

Simulations were carried out for a number of fcc and hcp crystals of different size and shape. In the simulation we kept the center of mass of the system fixed. Without this constraint the mean-square particle displacement would become of order L^2 (L = boxlength) as $\lambda \to 0$, in which case the integrand in Eq. (6) would be sharply peaked around $\lambda = 0$. This would have an adverse effect on the accuracy of the numerical integration. In contrast, with the center of mass fixed, $\langle r^2\rangle$ tends to $\langle r^2\rangle_0$, as $\lambda \to 0$, and no problems occur. The fixed center of mass MC was implemented as follows. The coordinates of all particles were expressed relative to the center of the periodic box. During a trial move a particle displacement over a distance $\Delta \mathbf{r}$ is attempted. As the intermolecular interactions depend only on relative distances the tests for particle overlaps can be carried out without knowledge of the position of the center of mass. In contrast, in order to compute $V = \lambda \sum_{i=1}^{N} (\mathbf{r}_i - \mathbf{r}_i^0)^2$, one needs to know the absolute position of each particle with respect to the reference lattice. The distance $\mathbf{r}_i - \mathbf{r}_i^0$ can be written as $\mathbf{r}_i^{(B)} - \mathbf{r}_i^{0(B)} - (\mathbf{R}_{CM}^{(B)} - \mathbf{R}_{CM}^{0(B)})$, where the superscript (B) indicates coordinates relative to the center of the periodic box; $\mathbf{R}_{CM}^{(B)}$ is the position of the center of mass in these units. In order to compute $\mathbf{r}_i - \mathbf{r}_i^0$ we have to keep track of the displacement $(\mathbf{R}_{CM}^{(B)} - \mathbf{R}_{CM}^{0(B)})$. This is a simple matter; every time a particle is moved from $\mathbf{r}^{(B)} \to \mathbf{r}^{(B)} + \Delta \mathbf{r}$, $\mathbf{R}_{CM}^{(B)}$ changes to $\mathbf{R}_{CM}^{(B)} + \Delta \mathbf{r}/N$. Note that changing the box coordinate of one particle implies changing the absolute coordinates of all particles in order to keep the center of mass fixed. Keeping the center of mass of the system fixed reduces the partition function by a factor V (in the limit $\lambda = 0$). Hence, the free energy per particle in the fixed center of mass solid is $(\ln V)/N$ higher than in the unconstrained system. We have corrected our data for this effect; all final results refer to hard-sphere solids with unconstrained center of mass. In order to compare fcc and hcp crystals of the same size and shape, we chose the shape of the periodic box such that the basal plane (x–y plane) was parallel to a set of close-packed planes [e.g., the fcc (111) plane]. The height of the box was chosen such that a multiple of six close-packed planes fitted in the box. For hcp and fcc crystal structures only the stacking of these planes differs: *ABABAB*... stacking for hcp and *ABCABC*... stacking for fcc. In addition, we performed a number of simulations at $\rho/\rho_0 = 0.7360$ with fcc crystals of different sizes in a cubic box with edges parallel to the crystallographic 100,010, and 001 axes. All Monte Carlo data are collected in Table I. In order to compute the free energy of an N–particle hard-sphere crystal we first evaluated the free energy of the interacting Einstein crystal with fixed center of mass, at $\lambda_{\max}$. This free energy contains three contributions: (i) the free energy of the corresponding noninteracting Einstein crystal, (ii) the virial contribution described in the Appendix, and (iii) a small correction to the virial contribution, which is also described in the Appendix; for the simulations with $\rho/\rho_0 = 0.7778$ this correction turned out to be negligible. The free energy of the unconstrained hard-sphere solid is then obtained by adding ΔF [Eq. (6)], together with a term $(\ln V)/N$ to account for the contribution of the center of mass motion to the free energy of the solid. Finally we compute the excess free energy F_{ex}^N, i.e., the free energy difference between the N-particle hard-sphere solid and an ideal gas with the same number of particles at the same density. All different contributions have been collected in Table I. In order to obtain the free energies of the different solid phases in the thermodynamic limit, we have to extrapolate to infinite system size. This extrapolation is not straightforward because we observe that the excess free energy depends not just on the number of particles, but also on the box shape. For instance, there is no significant difference between the excess free energy of a 54 ($= 3\times3\times6$) particle system and a 108 ($= 3\times3\times12$) particle system. But the excess free energy of the latter system *does* differ significantly from the corresponding value for the 108 particle system in a *cubic* box. We observed, however, that the excess free energy is a reasonably smooth function of $v_{\max}^{-1}$, where $v_{\max}$ is the volume of the largest cubic box that fits into the periodic box (see Fig. 1). For a cubic box $v_{\max}$ equals the total box volume, for all other shapes $v_{\max} = (L_{\min})^3$, where $L_{\min}$ is the shortest diameter of the box. Clearly for fixed box shape extrapolating as a function of $v_{\max}$ is equivalent to extrapolating as a function of N. We considered two types of extrapolation viz., $F_{ex}^{\infty} - F_{ex}^N \sim 1/v_{\max}$ and $F_{ex}^{\infty} - F_{ex}^N \sim (\ln v_{\max})/v_{\max}$, which correspond to $1/N$ and $(\ln N)/N$ extrapolations for fixed box shape. The results for the different extrapolation procedures have been collected in Table II. In most cases we find that the $1/v_{\max}$ extrapolation fits marginally better to the MC data than the $(\ln v_{\max})/v_{\max}$ extrapolation. In Table II we have also included the extrapolated values for the free energy difference $F_{ex}^{\infty}(\text{hcp}) - F_{ex}^{\infty}(\text{fcc})$.

Let us first look at the fcc data at $\rho/\rho_0 = 0.7360$. From the data shown in Table II it is clear that the nature of the extrapolation procedure is the major source of uncertainty in the final result. This is probably made worse by the fact that we have combined the results for a number of different box shapes. At $\rho/\rho_0 = 0.7778$, where we have studied systems with rather similar box shapes, the different extrapolations yield more consistent results. The present values for the excess free energy of the fcc solid at $\rho/\rho_0 = 0.7360$ agree well with the Hoover and Ree value[5]

$$F_{ex}^{\infty}(\text{fcc}) = 5.924(15).$$

Next we turn to the hcp solid at the same density. The extrapolated values for $F_{ex}^{\infty}(\text{hcp})$ have also been collected in

Notes on p. 113

TABLE I. Contributions to the excess free energy of an N-particle hard-sphere solid. N-number of particles, fcc/hcp—crystal structure of the solid under consideration. $N_x \times N_y$—number of atoms in a close-packed plane, N_z—number of stacked close-packed planes. Three simulations on the fcc solid at $\rho/\rho_0 = 0.7360$ were carried out in a cubic box, as indicated in the table. F^N_{Einst}—free energy of noninteracting Einstein crystal with fixed center of mass and spring constant $\lambda_{\max}$ ($\lambda_{\max} = 632.026$ at $\rho/\rho_0 = 0.7360$, $\lambda_{\max} = 1774.927$ at $\rho/\rho_0 = 0.7778$). All free energies in this table are expressed per particle. ΔF_{vir}—virial correction to the free energy of an Einstein crystal [Eq. (A6)]. ΔF_{corr}—correction to virial correction (see the Appendix). ΔF_{MC}—Monte Carlo result for the free energy difference between a hard-sphere solid and an interacting Einstein crystal (spring constant $\lambda_{\max}$) at the same density, both systems with fixed center of mass. $F^N_{\text{i.d.gas}}(\rho)$—free energy of an N-particle ideal gas at density ρ. F^N_{excess}—free energy difference between an N-particle hard-sphere solid and an ideal gas with the same number of particles at the same density. $F^N_{\text{excess}} = F^N_{\text{Einst}} + \Delta F_{\text{vir}} - \Delta F_{\text{corr}} + \Delta F_{\text{MC}} - F^N_{\text{i.d.gas}}(\rho) - (\ln V)/N$. ρ/ρ_0—(density)/(density at close packing). The error in the last two digits is indicated in brackets.

N	Type	$N_x \times N_y \times N_z$	F^N_{Einst}	ΔF_{vir}	ΔF_{corr}	ΔF_{MC}	$F^N_{\text{i.d.gas}}(\rho)$	F^N_{excess}	ρ/ρ_0
54	fcc	3×3 ×6	7.9198	0.0183	1.5×10^{-3}	−2.8929(39)	−0.9060	5.8766(39)	0.7360
54	hcp	3×3 ×6	7.9198	0.0183	2.2×10^{-3}	−2.8976(42)	−0.9060	5.8712(42)	0.7360
108	fcc	3×3 ×12	7.9477	0.0183	6.0×10^{-4}	−2.9722(08)	−0.9275	5.8799(08)	0.7360
108	hcp	3×3 ×12	7.9477	0.0183	1.2×10^{-3}	−2.9729(07)	−0.9275	5.8787(07)	0.7360
72	fcc	3×4 ×6	7.9349	0.0183	1.7×10^{-3}	−2.9190(28)	−0.9175	5.8912(28)	0.7360
72	hcp	3×4 ×6	7.9349	0.0183	2.5×10^{-3}	−2.9205(24)	−0.9175	5.8889(24)	0.7360
96	fcc	4×4 ×6	7.9447	0.0183	1.5×10^{-3}	−2.9364(30)	−0.9266	5.9047(30)	0.7360
96	hcp	4×4 ×6	7.9447	0.0183	1.5×10^{-3}	−2.9335(30)	−0.9266	5.9076(30)	0.7360
192	fcc	4×4 ×12	7.9559	0.0183	1.5×10^{-3}	−2.9841(30)	−0.9415	5.9030(30)	0.7360
192	hcp	4×4 ×12	7.9559	0.0183	1.5×10^{-3}	−2.9825(30)	−0.9415	5.9046(30)	0.7360
216	fcc	6×6 ×6	7.9568	0.0183	2.4×10^{-3}	−2.9754(10)	−0.9432	5.9159(10)	0.7360
216	hcp	6×6 ×6	7.9568	0.0183	8.0×10^{-4}	−2.9761(09)	−0.9432	5.9168(09)	0.7360
32	fcc	cubic box	7.8701	0.0183	8.0×10^{-4}	−2.7933(30)	−0.8771	5.8644(30)	0.7360
108	fcc	cubic box	7.9477	0.0183	7.0×10^{-4}	−2.9403(30)	−0.9298	5.9117(30)	0.7360
256	fcc	cubic box	7.9577	0.0183	1.7×10^{-3}	−2.9776(21)	−0.9455	5.9208(21)	0.7360
72	fcc	3×4 ×6	9.4623	0.0006	···	−3.7710(33)	−0.8622	6.4960(33)	0.7778
72	hcp	3×4 ×6	9.4623	0.0006	···	−3.7639(33)	−0.8622	6.5031(33)	0.7778
144	fcc	4×6 ×6	9.4909	0.0006	···	−3.8165(26)	−0.8811	6.5223(26)	0.7778
144	hcp	4×6 ×6	9.4909	0.0006	···	−3.8125(21)	−0.8811	6.5263(21)	0.7778
576	fcc	6×8 ×12	9.5052	0.0006	···	−3.8575(12)	−0.8976	6.5351(12)	0.7778
576	hcp	6×8 ×12	9.5052	0.0006	···	−3.8551(11)	−0.8976	6.5375(11)	0.7778
1152	fcc	8×12×12	9.5061	0.0006	···	−3.8637(15)	−0.9008	6.5375(15)	0.7778
1152	hcp	8×12×12	9.5061	0.0006	···	−3.8652(10)	−0.9008	6.5363(10)	0.7778

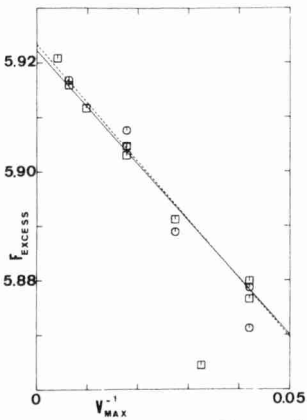

FIG. 1. System size dependence of the excess free energy of fcc (open squares) and hcp (open circles) hard-sphere solids at a reduced density $\rho/\rho_0 = 0.7360$. The excess free energy is in reduced units ($kT = 1$). The system size is characterized by the volume $v_{\max}$ of the largest cube that fits in the periodic box (see the text); the unit of volume is σ^3. Note that the excess free energy appears to be a smooth function of $v_{\max}^{-1}$ for all but the smallest system sizes even though this figure displays results of simulations on boxes of widely different shape. The drawn line is the best fit of F^N_{excess}(fcc) to an expression of the form $F^N_{ex} = F^\infty_{ex} - a/v_{\max}$. The dashed line is the corresponding fit to the HCP data. The intercepts and regression coefficients for these and other fits have been collected in Table II.

Table II. Note that for both extrapolations the difference in excess free energy between hcp and fcc is very small: 0.0012(14) and 0.0015(15) for the $1/v_{\max}$ and $(\ln v_{\max})/v_{\max}$ extrapolations respectively. Of course, we can also *first* compute ΔF^N, the free energy difference between corresponding hcp and fcc systems, and *then* exrapolate to the thermody-

TABLE II. Estimate of the excess free energy (per particle) of the hard-sphere fcc and hcp solids at infinite system size. The nature of the $1/v_{\max}$ and $(\ln v_{\max})/v_{\max}$ extrapolations are discussed in the text. As a measure for the quality of the extrapolation procedure the regression coefficient R is also shown. F^∞_{ex}(hcp) − F^∞_{ex}(fcc)—difference between the extrapolated excess free energies. [F(hcp)F(fcc)]$^\infty$—extrapolated free energy difference, i.e., $\lim_{N\to\infty} \Delta F^N$ (see the text). The error in the last two digits is indicated between brackets.

$\rho/\rho_0 = 0.7360$	$1/v_{\max}$ extrapolation	R	$(\ln v_{\max})/v_{\max}$ extrapolation	R
F^∞_{ex}(fcc)	5.9222(10)	0.97	5.9284(11)	0.97
F^∞_{ex}(hcp)	5.9234(10)	0.996	5.9299(12)	0.996
F^∞_{ex}(hcp) − F^∞_{ex}(fcc)	0.0012(14)	···	0.0015(15)	···
[F(hcp) − F(fcc)]$^\infty$	0.0017(14)	0.74	0.0021(17)	0.72
$\rho/\rho_0 = 0.7778$	$1/v_{\max}$ extrapolation	R	$(\ln v_{\max})/v_{\max}$ extrapolation	R
F^∞_{ex}(fcc)	6.5397(09)	0.97	6.5417(10)	0.94
F^∞_{ex}(hcp)	6.5404(11)	0.999	6.5436(13)	0.991
F^∞_{ex}(hcp) − F^∞_{ex}(fcc)	0.0007(14)	···	0.0019(16)	···
[F(hcp) − F(fcc)]$^\infty$	−0.0004(14)	0.79	−0.0011(16)	0.84

namic limit. This procedure is not quite equivalent to the previous one, because different data points have different statistical weights. Due to a cancellation of N-dependent contributions ΔF^N will be much less strongly N dependent than F_{ex}^N. If we assume that there is no systematic number dependence in ΔF^N we obtain $\Delta F^\infty = \langle \Delta F^N \rangle = 0.0001(8)$. Assuming a $1/v_{max}$ or a $(\ln v_{max})/v_{max}$ dependence of ΔF^N, yields $\Delta F^\infty = 0.0017(14)$ and $\Delta F^\infty = 0.0021(17)$, respectively. The extrapolated excess free energies of the hcp and fcc hard-sphere solid at $\rho/\rho_0 = 0.7778$ have been collected in the lower half of Table II. The corresponding differences between the hcp and fcc free energies are $F_{ex}^\infty(\text{hcp}) - F_{ex}^\infty(\text{fcc}) = 0.0007$ ($1/v_{max}$ extrapolation) and $F_{ex}^\infty(\text{hcp}) - F_{ex}^\infty(\text{fcc}) = 0.0019(16)$ [$(\ln v_{max})/v_{max}$ extrapolation]. Once again we can perform subtraction and extrapolation in reverse order. In that case we obtain for ΔF^∞: 0.0012(11) (no number dependence), $-0.0004(14)$ ($1/v_{max}$) and $-0.0011(16)$ [$(\ln v_{max})/v_{max}$]. As before, the free energy difference is very small. At neither density is the free energy difference between hcp and fcc solids significantly different from zero. The upper bound on the free energy difference is once again largely determined by the uncertainty in the extrapolation procedure. If we assume that the procedure in which ΔF^N is extrapolated to its infinite-system value is least error prone (it involves the smallest number of assumptions), we conclude that the free energy difference between hcp and fcc hard-sphere solids close to melting is most likely in the interval $-0.001 < \Delta F^\infty < 0.002$, where we have lumped the results at both densities together. Note that the simulations at $\rho/\rho_0 = 0.7778$, which were performed over a wide range of system sizes (between $N = 72$ and $N = 1152$), suggest that there is a pronounced system size dependence of the free energy difference ΔF^N (see Fig. 2). We are not aware of other direct computations of the hcp–fcc free energy difference close to melting. However, several estimates exist for densities at or near close packing. For instance, Alder, Hoover, and Young[13] conclude that at close packing $|\Delta F^\infty| < 0.04$. In later work by Alder, Carter and Young[14] and Alder, Young, Mansigh, and Salzburg[10] the free energy difference between hcp and fcc at close packing is estimated to be $\Delta F^\infty = 0.002$. More recent work by Kratky[11] yields a much higher estimate of this free energy difference, viz, $\Delta F^\infty = 0.021(5)$ at $\rho/\rho_0 = 0.995$. This value is much larger than the earlier estimates, but fairly close to the free-volume prediction $\Delta F^\infty = 0.015(9)$. The present result is compatible with the results of Alder *et al.* but it appears to be incompatible with Kratky's value because if both the present results and the results of Ref. 11 were correct, this would imply that the pressure difference $\Delta P = P_{hcp} - P_{fcc}$ must be, on average, $\Delta P = 0.05$ between melting and close packing. This relatively large pressure difference is larger than the upper bound for ΔP that follows from the MD results of Refs. 10 and 13. It should be noted that in view of the very small free energy difference between hcp and fcc phases, the true state of lowest free energy at densities below close packing must contain stacking faults (i.e., stacking of the type *ABACBCABA*...). Of course, the contribution to the free energy due to this kind of disorder vanishes in the thermodynamic limit.

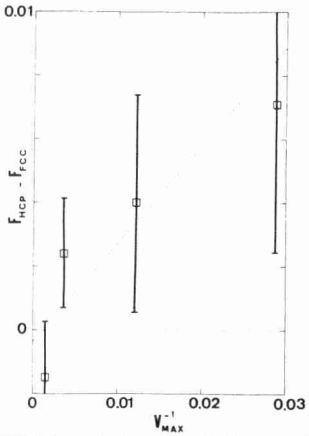

FIG. 2. System size dependence of the free energy difference between hcp and fcc hard-sphere solids of the same size and shape at a reduced density $\rho/\rho_0 = 0.7778$. Although the error bars on these data points are relatively large (but quite small in an absolute sense), the data suggest that the hcp–fcc free energy difference ΔF^N is strongly system size dependent. The dashed line is a fit to the MC data of the form $\Delta F^N = \Delta F^\infty - a'/v_{max}$. The intercept and regression coefficient for this fit are quoted in Table II. Units are as in Fig. 1.

CONCLUSION

In this paper we have developed a new method to compute the absolute free energy of arbitrary solid phases. The method is fast and accurate, and can also be applied to molecular solids[15] and solids containing defects. The basic idea is to constrict a reversible path between the solid under consideration and an Einstein crystal with the same structure. In the previous section we have demonstrated the conceptually simplest but numerically least sophisticated example of this method, namely one in which the spring constants are switched on while the intermolecular interations remain unaffected. For continuous intermolecular potentials the method may be expected to work much better if the intermolecular forces are swtiched off while the spring constant are being switched on, in such a way that the mean-square particle displacement remains approximately constant for all values of λ. Even for hard-core interactions it is easy to find a well behaved, nonlinear parametrization of the Hamiltonian which yields the unperturbed Hamiltonian at $\lambda = 0$ and the perfect Einstein crystal at $\lambda = \lambda_{max}$.

ACKNOWLEDGMENTS

This work was started at a CECAM workshop on transport in molecular fluids at Orsay, France in the summer of 1983. We thank Dr. Moser for creating the conditions which made this work possible; we thank the attendants of the workshop for many stimulating discussions.

APPENDIX

In this Appendix we derive an approximate expression for the free energy of an interacting Einstein crystal, which

Notes on p. 113

becomes exact at sufficiently high values of the spring constant λ. The configurational part of the partition function of the interacting Einstein crystal is of the following form:

$$Q(T;\lambda) = \int \cdots \int \exp\left[-\beta\lambda \sum_i (\Delta \mathbf{r}_i)^2\right] \exp\left[-\beta \sum_{i<j} u(r_{ij})\right] d\mathbf{r}^N, \tag{A1}$$

where $\Delta \mathbf{r}_i = \mathbf{r}_i - \mathbf{r}_i^0$ ($\mathbf{r}_i^0$ is the lattice site of particle i), $\beta = 1/kT$ and $u(r_{ij})$ is the value of the pair potential of particles i and j at separation r_{ij}. Equation (A1) can be rewritten as

$$Q(T;\lambda) = Q_E(T;\lambda)\left\langle \exp\left[-\beta \sum_{i<j} u(r_{ij})\right]\right\rangle_E, \tag{A2}$$

where $Q_E(T;\lambda)$ is the partition function of the noninteracting Einstein crystal with spring constant λ. The subscript E in Eq. (A2) stands for averaging over all configurations of the noninteracting Einstein crystal. Such an average can, in principle, be carried out by Monte Carlo (umbrella sampling) but in the present case we use an expansion in cluster functions $f_{ij} = \{\exp[-\beta u(r_{ij})] - 1\}$:

$$\left\langle \exp\left[-\beta \sum_{i<j} u(r_{ij})\right]\right\rangle_E = \left\langle 1 + \sum_{i<j} f_{ij} + \sum_{i<j}\sum_{k<l} f_{ij} f_{kl} + \cdots \right\rangle_E. \tag{A3}$$

Note that for hard spheres $-\langle f_{ij}\rangle = \langle P^{ij}_{\text{overlap}}\rangle$, the probability that particles i and j in the noninteracting Einstein crystal are separated by a distance $|\mathbf{r}_{ij}| < \sigma$. At high values of λ all $\langle f_{ij}\rangle$ for i and j not nearest neighbors become negligible, while $|\langle f_{ij}^{nn}\rangle| \ll 1$ (nn stands fo. "nearest neighbors"). In this limit we may approximate Eq. (A3) by

$$\left\langle \exp\left[-\beta \sum_{i<j} u(r_{ij})\right]\right\rangle_E \simeq (1 + \langle f_{ij}^{nn}\rangle)^{Nn/2}. \tag{A4}$$

In Eq. (A4) n stands for the number of nearest neighbors of a particle i (for both hcp and fcc solids $n = 12$). To the same level of approximation $\langle f_{ij}^{nn}\rangle$ can be evaluated by computing the probability of overlap of two isolated harmonically bound penetrating spheres of diameter σ at an average separation $a = |r_i^0 - r_j^0|$. This probability can be evaluated analytically. The result is

$$\langle P^{nn}_{\text{overlap}}\rangle_\lambda = \tfrac{1}{2}\{\text{erf}[(\beta\lambda/2)^{\frac{1}{2}}(\sigma + a)] + \text{erf}[(\beta\lambda/2)^{\frac{1}{2}}(\sigma - a)]\} - \{\exp[-\beta\lambda(\sigma - a)^2/2] - \exp[-\beta\lambda(\sigma + a)^2/2]\}/[(2\pi\beta\lambda)^{\frac{1}{2}} a]. \tag{A5}$$

The expression which relates the free energy of the interacting Einstein crystal to that of a noninteracting Einstein crystal F_E then becomes

$$F(T;\lambda) = F_E(T;\lambda) - N(n/2)kT \ln(1 - \langle P^{nn}_{\text{overlap}}\rangle_\lambda). \tag{A6}$$

From this expression for $F(T;\lambda)$ we can derive an estimate for the mean-square particle displacement in the interacting Einstein crystal ($\langle r^2\rangle_\lambda = -N^{-1}(\partial F/\partial\lambda)$):

$$\langle r^2\rangle_\lambda = \langle r^2\rangle_E - (\beta n/2)\frac{\{[\sigma a - \sigma^2 - (\beta\lambda)^{-1}]\exp[-\tfrac{1}{2}\beta\lambda(a-\sigma)^2] + (\sigma a + \sigma^2 - (\beta\lambda)^{-1})\exp[\tfrac{1}{2}\beta\lambda(a+\sigma]^2)\}}{2a(2\pi\beta\lambda)^{\frac{1}{2}}(1 - \langle P^{nn}_{\text{overlap}}\rangle_\lambda)}. \tag{A7}$$

In Eq. (A7) $\langle r^2\rangle_E$ stands for the mean-square particle displacement in the nonintracting Einstein crystal. The second term on the right-hand side is the correction due to hard-core interactions. The above expression for the mean-square particle displacement in the interacting Einstein crystal can be compared directly to Monte Carlo results at high values of λ. In fact, our choice of $\lambda_{\max}$ [see Eq. (6)] was dictated by the requirement that the mean-square particle displacement at $\lambda_{\max}$ obeyed Eq. (A7). On closer scrutiny of the MC results we found that the MC results for the simulations at $\rho/\rho_0 = 0.7360$, $\lambda = 632.026$ still deviated slightly [$0(10^{-5})$] from Eq. (A7). However, it was found that this difference $\Delta = \langle r\rangle_\lambda^{MC} - \langle r^2\rangle_\lambda^{vir}$ {the superscript "vir" stands for the "virial" expression [Eq. (A7)]} depends exponentially on λ: $\Delta = \alpha \exp(-\lambda/\delta)$ with $\alpha = 0(10^{-3})$ and $\delta = 0(10^2)$. As a consequence, Eq. (A6) overestimates the free energy of the interacting Einstein crystal by an amount $\Delta F_{\text{corr}} = \int_{\lambda_{\max}}^{\infty} \Delta\, d\lambda = \alpha\lambda_{\max}\exp(-\lambda_{\max}/\delta)$. This correction, which turned out to be of the same order as the estimated error in the free-energy integration [Eq. (6)] was taken into account in the evaluation of the free energy of the hard-sphere solid. At $\rho/\rho_0 = 0.7778$, $\lambda_{\max} = 1774.927$ ΔF_{corr} was negligible. Finally, we also corrected for the fact that in the Monte Carlo simulations we kept the center of mass of the system fixed. Hence, our reference state is not the normal Einstein crystal, but an Einstein crystal with fixed center of mass. The partition function of an Einstein crystal with fixed center of mass is given by

$$Q'_E(T;\lambda) = N^{-3/2}(\pi/\beta\lambda)^{3(N-1)/2}. \tag{A8}$$

Similarly, the state at $\lambda = 0$ in our simulation was not the normal hard-sphere solid, but a hard-sphere solid with fixed center of mass. The partition function of the latter system differs from the partition function of the former by a factor V^{-1}.

[1] M. Parinello and A. Rahman, Phys. Rev. Lett. **45**, 1196 (1980), J. Appl. Phys. **52**, 7182 (1981).
[2] D. Levesque, J.-J. Weis, and M. L. Klein, Phys. Rev. Lett. **51**, 670 (1983).
[3] M. Parinello, A. Rahman and P. Vashishta, Phys. Rev. Lett. **50**, 1073 (1983).
[4] W. G. Hoover and F. H. Ree, J. Chem. Phys. **47**, 4873 (1967).
[5] W. G. Hoover and F. H. Ree, J. Chem. Phys. **49**, 3609 (1968).
[6] H. Ogura, H. Matsuda, T. Ogawa, N. Ogita, and U. Ueda. Prog. Theor. Phys. **58**, 419 (1977).
[7] W. G. Hoover, S. C. Gray, and K. Johnson, J. Chem. Phys. **55**, 1128 (1971).
[8] J. P. Valleau and G. M. Torrie in *Statistical Mechanics A, Modern Theoretical Chemistry*, edited by B. J. Berne (Plenum, New York, 1977), Vol. 5, p. 178.
[9] D. A. Young and B. J. Alder, J. Chem. Phys. **60**, 1254 (1974).
[10] B. J. Alder, D. A. Young, M. R. Mansigh, and Z. W. Salzburg, J. Comp. Phys. **7**, 361 (1971).
[11] K. W. Kratky, Chem. Phys. **57**, 167 (1981).
[12] M. Abramowitz and I. A. Stegun, *Handbook of Mathematical Functions* (Dover, New York, 1970).
[13] B. J. Alder, W. G. Hoover and D. A. Young, J. Chem. Phys. **49**, 3688 (1968).
[14] B. J. Alder, B. P. Carter, and D. A. Young, Phys. Rev. **183**, 831 (1969).
[15] D. Frenkel and B. M. Mulder (to be published).

Notes to Reprint II.4

1. The method described in this paper was later extended to continuous potentials (see Reprint IV.8).

2. Reference [15] was later published as (Frenkel and Mulder, Mol. Phys. 55 (1985) 1171).